

Article

# Characteristics and Expression Analysis of *FmTCP15* under Abiotic Stresses and Hormones and Interact with DELLA Protein in *Fraxinus mandshurica* Rupr.

Nansong Liang<sup>1,2</sup>, Yaguang Zhan<sup>1,2,\*</sup> , Lei Yu<sup>1,2</sup>, Ziqing Wang<sup>1,2</sup> and Fansuo Zeng<sup>1,2</sup>

<sup>1</sup> State Key Laboratory of Tree Genetics and Breeding, Northeast Forestry University, Harbin 150040, China; liangnansong@nefu.edu.cn (N.L.); leiyunefu@126.com (L.Y.); wangziqing1001@126.com (Z.W.); youpractise@126.com (F.Z.)

<sup>2</sup> Department of Forest Bioengineering, Northeast Forestry University, Harbin 150040, China

\* Correspondence: zhanyaguang2014@126.com; Tel.: +86-0451-8219-1752

Received: 10 March 2019; Accepted: 14 April 2019; Published: 17 April 2019



**Abstract:** The TEOSINTE BRANCHED1, CYCLOIDEA, and PROLIFERATION CELL FACTOR (TCP) transcription factor is a plant-specific gene family and acts on multiple functional genes in controlling growth, development, stress response, and the circadian clock. In this study, a class I member of the TCP family from *Fraxinus mandshurica* Rupr. was isolated and named *FmTCP15*, which encoded a protein of 362 amino acids. Protein structures were analyzed and five ligand binding sites were predicted. The phylogenetic relationship showed that *FmTCP15* was most closely related to Solanaceae and Plantaginaceae. *FmTCP15* was localized in the nuclei of *F. mandshurica* protoplast cells and highly expressed in cotyledons. The expression pattern revealed the *FmTCP15* response to multiple abiotic stresses and hormone signals. Downstream genes for transient overexpression of *FmTCP15* in seedlings were also investigated. A yeast two-hybrid assay confirmed that *FmTCP15* could interact with DELLA proteins. *FmTCP15* participated in the GA-signaling pathway, responded to abiotic stresses and hormone signals, and regulated multiple genes in these biological processes. Our study revealed the potential value of *FmTCP15* for understanding the molecular mechanisms of stress and hormone signal responses.

**Keywords:** molecular cloning; functional analysis; TCP; DELLA; GA-signaling pathway; *Fraxinus mandshurica* Rupr.

## 1. Introduction

The survival of plants requires balancing the regulation of growth, development, and stress response. Plants need to utilize many mechanisms to respond to stress, while environmental changes may affect development. A large number of complex transcription factors (TFs) and genes are required and involved, and there is a novel TF family that participates in these processes.

The TEOSINTE BRANCHED1, CYCLOIDEA, and PROLIFERATION CELL FACTOR (TCP) gene family is a plant-specific TF family that was first identified in 1999. TCP is named after the first three identified members: *TEOSINTE BRANCHED1* (*tb1*) in maize (*Zea mays*), *CYCLOIDEA* (*CYC*) in snapdragon (*Antirrhinum majus*), and the *PROLIFERATING CELL FACTORS 1* and *2* (*PCF1* and *PCF2*) in rice (*Oryza sativa*) [1–3]. The TCP gene family encodes a 59-amino-acid residue, noncanonical basic helix-loop-helix (bHLH) motif called the TCP domain, which allows DNA binding and protein–protein interactions [3–5]. Based on the differences between the TCP domains, the TCP family was divided into two major classes: class I (also known as PCF or TCP-P) and class II (also known as TCP-C) [6–8]. Class II was further divided into two clades, named CINCINNATA (*CIN*) [9] and CYCLOIDEA/TEOSINTE BRANCHED1(*CYC/TB1*) [5,10].

Class I TCP genes have been reported to promote plant growth and proliferation. In meristematic tissues, *PCF1/PCF2* from rice and *AtTCP20* from *Arabidopsis thaliana* act as transcriptional activators of *PCNA* and *CYCB1;1*, respectively [3,11]. However, the latest research indicates that class I TCP genes also participate in stress adaptation. In rice, *OsPCF2* positively regulates the *OsNHX1* gene by binding to its promoter and responds to salt and drought stress tolerance [12]. *OsTCP19* responds to water deficit and salt stress and interacts with *OsABI4* and *OsULT1* to function in abiotic stress response and abscisic acid (ABA) signaling [13]. The CIN clade of class II is mainly involved in regulating organ development, such as floral organ, leaf, and lateral organ development [14–17]. In *Arabidopsis*, CIN is required for the arrest of cell division in the peripheral regions of the leaf. *jaw-D* mutants, *cin* loss-of-function mutants, in which *TCP2*, *TCP3*, *TCP4*, *TCP10*, and *TCP24* were all strongly reduced, achieved highly crinkled leaves [14]. The CYC/TB1 clade of class II is mainly involved in regulating shoot branching, floral transition, organ identity, and development. In *Arabidopsis*, one of TCP family members, *BRANCHED1* (*BRC1*), is expressed in axillary buds and responds to endogenous and environmental signals and leads to branch suppression [18,19]. In rice, *OsTB1* interacts with *OsMADS57* and targets *Dwarf14* (*D14*) to control the outgrowth of axillary buds [20]. It is noteworthy that the two different classes of TCPs are believed to share common targets [21]. In *Arabidopsis*, *LIPOXYGENASE 2* (*LOX2*) was identified as a common target of *TCP20* (from class I) and *TCP4* (from class II); additionally, *TCP20* could inhibit but *TCP4* could induce the expression of *LOX2* [22]. These results show a proposed model by which classes I and II TCP proteins may act antagonistically. In tomato (*Solanum lycopersicum*), classes I and II SlTCP proteins can form homo- and heterodimers [23]. These results show a proposed model by which classes I and II TCP may act antagonistically and form functional protein complexes to regulate biological processes.

Although TCP gene functions have been shown to be responsive to both development and various stresses in model plants, their roles in forestry trees are less known. *Fraxinus mandshurica* Rupr., a member of the Oleaceae family, is a broad-leaved tree and is well known as the most valuable hardwood tree widely distributed in the conifer and hardwood mixed forest in northeastern China [24–26]. As an important economic and timber species, studies of *F. mandshurica* have mainly focused on its seed germination [27], nutritional growth [28], ecological characteristics [29], and disease control [30]. However, there have been few reports on the genes that contribute to resistance to abiotic stresses and development responses in *F. mandshurica*. In this study, *FmTCP15*, a class I TCP transcription factor, was isolated. The gene structure, phylogenetic relationship, subcellular localization, transcript levels in different tissues, expression under abiotic stresses and hormone signaling, as well as the expression of downstream genes of *FmTCP15* were analyzed. We found that *FmTCP15* was mainly induced by cold, salt and drought stress, and gibberellic acid (GA3). Overexpressing *FmTCP15* caused a significant change in the expression of a series of key genes involved in stress response and the GA-signaling pathway. Moreover, *FmTCP15* could interact with DELLA proteins (*FmRGA* and *FmGAI*), which are key proteins of the GA-signaling pathway. The interaction relationship between *FmTCP15* and DELLA proteins may enhance the ability of the plant to resist stresses. Therefore, we postulate that *FmTCP15* could regulate DELLA proteins at both transcriptional and post-transcriptional levels. *FmTCP15* may regulate stress genes and balance plant growth and development through the GA-signaling pathway.

## 2. Materials and Methods

### 2.1. Plant Material and Growth Conditions

*F. mandshurica* seeds from the Northeast Forestry University experimental forest farm were used. The seeds were surface sterilized and grown at 25 °C under long-day conditions (16 h light/8 h dark) on a standard field. For expression analysis, main root, lateral root, xylem, phloem, cotyledon, function leaves, and petiole were harvested from 30-day-old seedlings.

## 2.2. Cloning and Identification of *FmTCP15* Gene

The MiniBEST Plant RNA Extraction Kit (Takara Bio, Inc., Shiga, Japan) was used for total RNA extraction. The cDNA synthesized was created using the PrimeScript First Strand cDNA Synthesis Kit (Takara Bio Inc., Shiga, Japan). The full-length cDNA of *FmTCP15* was obtained by PCR using the primers *FmTCP15-F* (5'-ACCCATTCTTGAACCAACCTATC-3') and *FmTCP15-R* (5'-CCAAACCCTAAATCCTCCACAT-3'). The sequence of the *FmTCP15* gene was submitted to GenBank with the accession number KX905157.

## 2.3. Sequence Features, Protein Modeling, and Phylogenetic Analysis of *FmTCP15*

ProtParam was used for analysis of the physical and chemical properties (molecular mass and isoelectric point) (<http://web.expasy.org/protparam/>) [31]. TMpred was used for the prediction of transmembrane regions and orientation ([https://embnet.vital-it.ch/software/TMPRED\\_form.html](https://embnet.vital-it.ch/software/TMPRED_form.html)) [32]. The I-TASSER server was used to produce the protein model (<http://zhanglab.ccmb.med.umich.edu/I-TASSER/>) [33,34]. ModRefiner online software was further used to refine the protein model (<http://zhanglab.ccmb.med.umich.edu/ModRefiner/>) [35]. The NCBI database BLAST method (<https://blast.ncbi.nlm.nih.gov/Blast.cgi>) was used to search for homologous sequences of *FmTCP15*. Multiple sequence alignment was performed using CLC Genomics Workbench 12. The conserved domains of *FmTCP15* were analyzed by the NCBI Conserved Domain Database (<http://www.ncbi.nlm.nih.gov/Structure/cdd/cdd.shtml>). The phylogenetic tree was constructed by MEGA 5.0 with the neighbor-joining method and 1000 replicates of bootstrap analysis.

## 2.4. Subcellular Localization of *FmTCP15* Proteins

The *FmTCP15* coding region was introduced into the pROKII-GFP expression vector driven by the *CaMV-35S* promoter and fused to the 5' green fluorescence protein (GFP) gene to generate 35S::*FmTCP15*-GFP using the specific primers *pRTCP15-GFP-F* (5'-GGTACCGATAC TCGAGATGGAAGGATTAGGTGATGA-3') and *pRTCP15-GFP-R* (5'-CACGGGTCATCTCGAGTGA ATGGTGGTTCGTAGTC-3'). The constructed vector was transformed into *F. mandshurica* xylem protoplasts, which were isolated from xylem, as described for poplar protoplast constructs, with some modifications [36]. Fluorescence signals of the 35S::*FmTCP15*-GFP fusion protein were examined using a confocal microscope (Zeiss Confocal Microscopy, model LSM410, Zeiss, Jena, Germany).

## 2.5. Abiotic Stresses and Hormone Signal Treatments

Thirty-day-old *F. mandshurica* seedlings were selected and subjected to different abiotic stresses and hormone signaling treatments. For cold treatment, seedlings were transferred into liquid Murashige and Skoog (MS) medium and placed at 4 °C. For salt and drought stress treatments, seedlings were transferred into liquid MS medium, which contained 200 mm/L NaCl and 20% w/v PEG6000, respectively. For hormone treatment, seedlings were transferred into liquid MS medium containing 100 µmol/L ABA (abscisic acid) and 100 µmol/L GA3 (gibberellic acid), respectively. For control, untreated seedlings were transferred into liquid MS medium at 25 °C. The stresses and hormones were treated at 0, 6, 12, 24, 48, and 72 h.

## 2.6. Transient Overexpression of *FmTCP15* Gene

The constructed pROKII-GFP expression vector 35S::*FmTCP15*-GFP and empty vector pROKII-GFP were used in overexpression of *FmTCP15* and negative control plants, respectively, and the two vectors were transformed into *Agrobacterium tumefaciens*. Twenty-day-old *F. mandshurica* wild-type (WT) seedlings were used for transient transformation, which followed the method described for Birch (*Betula platyphylla* Suk.) [37]. After coculture with *Agrobacterium*, transient overexpression of the *FmTCP15* whole seedlings was collected.

### 2.7. Analysis of Gene Expression of *FmTCP15* and Downstream Genes

The quantified RNA was reverse-transcribed into cDNA using the PrimeScript™ RT reagent kit with gDNA Eraser (Perfect Real-Time) (Takara Bio Inc., Shiga, Japan). Quantitative RT-PCR (qRT-PCR) was conducted in a 7500 Real-Time PCR system (Applied Biosystems, Forster City, CA, USA) using the Takara SYBR® Premix Ex Taq™ II (Perfect Real Time) (Takara Bio, Inc., Shiga, Japan). All reactions were performed in triplicate to ensure technical and biological reproducibility, and the relative abundance of the transcripts was calculated using 7500 Software v 2.0.6 (Applied Biosystems, Forster City, CA, USA) using the comparative  $2^{-\Delta\Delta CT}$  method [38]. The qRT-PCR primer pairs are shown in Table S1. Tubulin was used as an internal control to determine the expression levels of the target genes.

### 2.8. Yeast Two-Hybrid Protein–Protein Interaction Assays

The yeast two-hybrid (Y2H) assay was carried out using the Matchmaker™ Gold Yeast Two-Hybrid System (Clontech Laboratories Inc., Mountain View, CA, USA). The full-length coding sequence of *FmTCP15* was recombined into the pGBKT7 (BD) bait vector and pGADT7 (AD) prey vector, respectively. The candidate downstream genes of *FmTCP15* were recombined into the pGADT7 (AD) vector. The gene-specific primers are listed in Table S2. The pGBKT7-p53xpGADT7-T and pGBKT7-lamxpGADT7-T were used as positive and negative controls, respectively. The plasmids of bait and prey vectors were co-transformed into the yeast strain Y2HGOLD by using the lithium acetate method. The self-activation ability of the bait vector was tested. The transformed strains were further serially cultured on selective media, including SD/-Leu/-Trp (DDO), SD/-Ade/-Leu/-Trp (TDO), SD/-Ade/-His/-Leu/-Trp/Aureobasidin A (AbA<sup>r</sup>) (QDO/A), and SD/-Ade/-His/-Leu/-Trp/AbAr/X- $\alpha$ -Gal (QDO/A/X) with 125  $\mu$ M AbA<sup>r</sup> and 4 mg mL<sup>-1</sup> X- $\alpha$ -Gal and incubated at 30 °C for 3–5 days.

## 3. Results

### 3.1. Nucleotide Sequence Cloning and Protein Modeling of *FmTCP15* Gene

The *Arabidopsis* AtTCP15 amino acid sequence was used to blast against the *F. mandshurica* TSA database. Then, we obtained the predicted cDNA sequence of the *AtTCP15* homologous gene in *F. mandshurica*. According to the sequence, specific primers were designed and the *FmTCP15* full-length cDNA sequence was obtained (GenBank: KX905157). The open reading frame (ORF) was 1089 bp and encoded a protein of 362 amino acids with a predicted molecular mass of 39.0 kDa and a theoretical isoelectric point (pI) of 6.67. The transmembrane prediction showed that the *FmTCP15* protein had four possible transmembrane helices, located at 29–53, 129–149, 255–279, and 294–310 aa, which indicated that the *FmTCP15* protein may have transmembrane capabilities. Secondary structure analysis of the *FmTCP15* protein revealed that *FmTCP15* consisted of  $\alpha$ -helix (65.54%), extended strand (5.78%), and random coil (28.67%). The conserved domains of the *FmTCP15* protein indicated that *FmTCP15* contained a TCP domain ranging from 75 to 136 aa and belonged to the class I TCP superfamily.

For three-dimensional (3D) structure modeling, the *FmTCP15* protein sequence was submitted to the I-TASSER server. The PDB template 2nbiA was used for homology modeling (identity 86.1%, coverage 93.9%). The *FmTCP15* protein model was achieved (Figure 1A,B). Then, using the COACH method, five ligand binding sites (THR117, GLU119, TRP120, LEU121, and LEU122) were predicted (Figure 1C,D). Next, based on homologous Gene Ontology (GO) templates in PDB, we predicted GO terms for the *FmTCP15* protein. The *FmTCP15* protein had molecular functions GO:0032559 and GO:0035639 (adenyl ribonucleotide binding and purine ribonucleotide triphosphate binding); biological processes GO:0044255, GO0032787, and GO:0046394 (cellular lipid metabolic process, monocarboxylic acid metabolic process, and carboxylic acid biosynthetic process); and cellular components GO:0032991 and GO:0044445 (macromolecular complex).

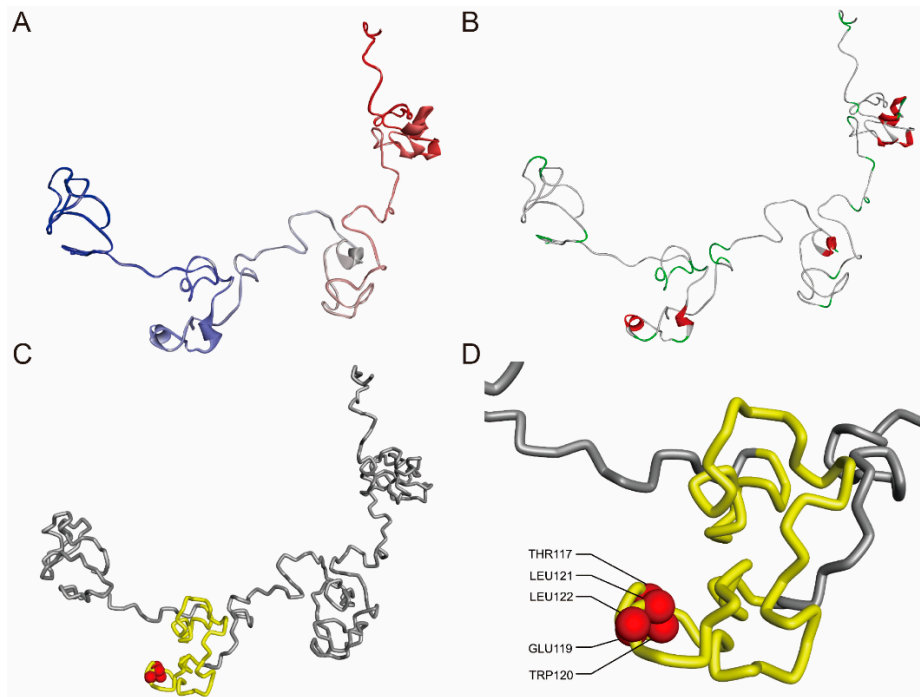


**Figure 1.** Three-dimensional protein model of FmTCP15 protein. (A) FmTCP15 3D structure displayed in solid ribbon style. N-to-C terminals: color residues in a continuous gradient from blue at the N-terminus through white to red at the C-terminus. (B) FmTCP15 3D structure displayed in solid ribbon style, secondary type: colors according to secondary structure. Helices are red, turns are green, and coils are white. (C) FmTCP15 3D structure displayed in tube style: the TCP domain is yellow, and the five predicted ligand binding sites (THR117, GLU119, TRP120, LEU121, and LEU122) are red balls. (D) The zoom-in view of the TCP domain of FmTCP15.

### 3.2. Homology Analysis and Phylogenetic Relationship of FmTCP15

For homologous alignment, FmTCP15 and 13 other amino acid sequences were aligned using CLC Genomics Workbench 12 (Table S3). The results revealed that the FmTCP15 shared high similarities with homologous genes from other species (Figure 2A). FmTCP15 and the 13 other genes shared a TCP conserved domain, and five ligand binding sites (THR117, GLU119, TRP120, LEU121, and LEU122) were also conserved in these species (Figure 2A).

To analyze the phylogenetic relationships between FmTCP15 and the homologous sequences of TCP15s in other plants, we constructed a phylogenetic tree. FmTCP15 and 42 other amino acid sequences were used for tree construction, including 34 dicotyledons, 7 monocotyledons, and 1 bryophyte (Table S4). The phylogenetic tree revealed a clear boundary between the TCP proteins of dicotyledons, monocotyledons, and bryophytes (Figure 2B). FmTCP15 was most closely related to the Solanaceae and Plantaginaceae families, such as CaTCP14 (*Capsicum annuum*, XP\_016562806.1), NtTCP14-like (*Nicotiana tabacum*, XP\_016464955.1), SlTCP17 (*Solanum lycopersicum*, NP\_001233815.1), SpTCP14-like (*Solanum pennellii*, XP\_015077184.1), StTCP14-like (*Solanum tuberosum*, XP\_006354786.1), and AmTCP (*Antirrhinum majus*, CAE45599.1). Together with OeTCP14-like (*Olea europaea* var. *sylvestris*, XP\_022844971.1), also an Oleaceae family protein, these nine sequences were grouped into one clade.



### 3.3. Subcellular Localization of *FmTCP15* Proteins

Subcellular localization is crucial for understanding protein function. To further investigate the subcellular localization of *FmTCP15*, we constructed *F. mandshurica* xylem protoplasts, which we observed with a confocal microscope after protoplast transformation with pROK2-*FmTCP15*-GFP vector (35S::*TCP15*-GFP). The results showed that the fluorescence signals were mainly concentrated in the nucleus, which demonstrated that *FmTCP15* was located in the nucleus (Figure 3).

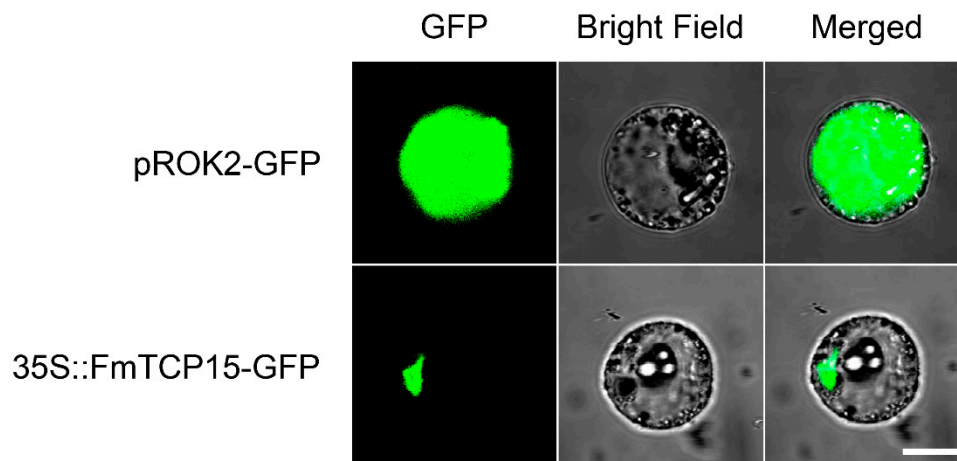


**Figure 3.** Subcellular localization of *FmTCP15*. The photographs were taken under darkfield illumination for green fluorescence localization (GFP), bright-field illumination to examine cell morphology (Bright field), and merged-field illumination (Merged). The bar represents 10  $\mu\text{m}$ .

### 3.4. Expression Pattern of *FmTCP15* in Different Tissues and Treatments

To determine the tissue-specific expression pattern of *FmTCP15*, we performed qRT-PCR in different tissues, including the main root, lateral root, xylem, phloem, cotyledon, function leaves, petiole, and seed. The expression level of *FmTCP15* was expressed highest in the cotyledons, followed by the xylem, and expressed lowest in the seeds (Figure 4A).

To investigate the expression pattern of *FmTCP15* under abiotic stresses and hormone signals, *F. mandshurica* seedlings were exposed to cold, salt, and drought stress treatments, as well as ABA and GA3 hormone signal. The results showed that, in response to abiotic stress treatment, *FmTCP15* gene expression was induced under cold, salt, and drought conditions (Figure 4B–F). However, the induction pattern was different. Cold stress induced *FmTCP15* to a high value from 6 to 12 h after initiation of the treatment, with a peak value at 12 h (Figure 4B). Salt stress induced *FmTCP15* to a peak value at 6 h after initiation of treatment (Figure 4C). In contrast, drought stress induced *FmTCP15* to a double peak expression pattern: the first peak value was at 6 h, and the second peak value was at 24 h (Figure 4D). For the hormone signal treatments, *FmTCP15* was downregulated after initiation of ABA treatment, with a double valley pattern: the first valley was at 24 h and the second valley was at 72 h (Figure 4E). GA3 induced *FmTCP15* expression, with a peak at 6 h (Figure 4F). These results indicate that *FmTCP15* responded to cold, salt, and drought abiotic stresses and ABA and GA3 treatments and imply that *FmTCP15* may participate in growth and development, as well as stress responses.

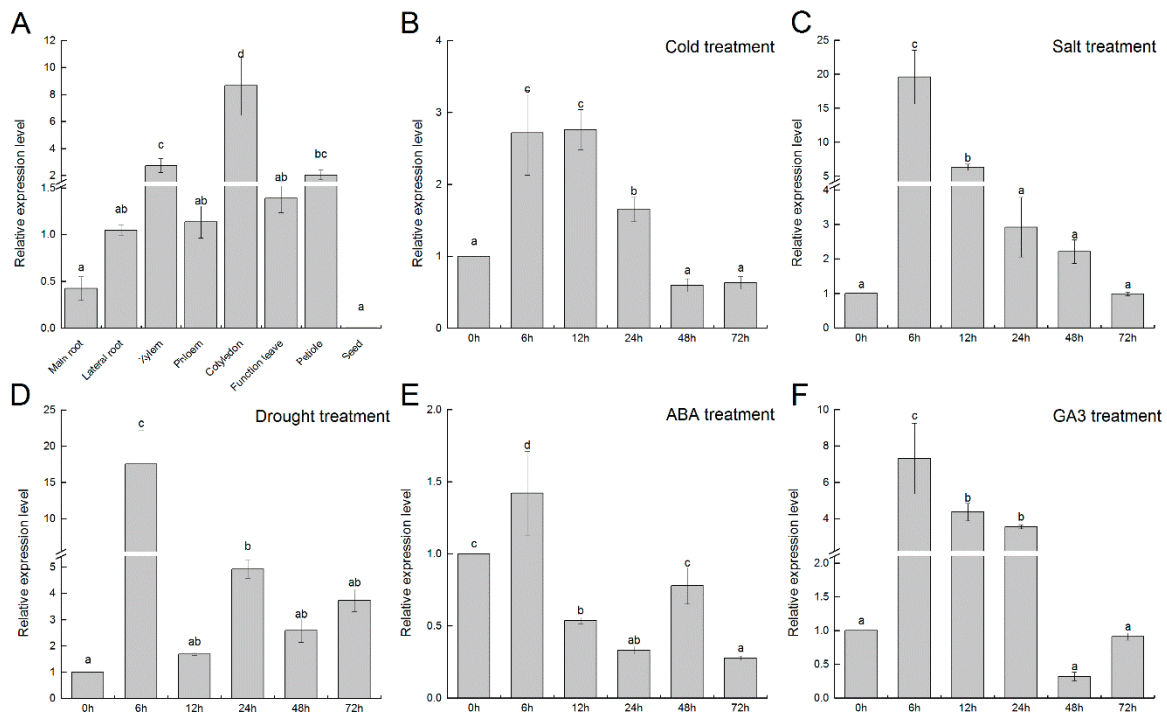


**Figure 4.** Expression patterns of *FmTCP15*. (A) Expression patterns of *FmTCP15* gene in different tissues. (B–F) Expression patterns of *FmTCP15* under different stress and hormone signal treatments: (B) cold (4 °C), (C) salt (200 mm/L NaCl), (D) drought (20% w/v PEG6000), (E) abscisic acid (100 µmol/L ABA), and (F) gibberellic acid (100 µmol/L GA3). Different letters above bars within statistically significant differences between different times of the treatments at the  $p < 0.05$  level according to Duncan's multiple range test.

### 3.5. Functional Assay of Transient Overexpression of *FmTCP15* in *F. mandshurica*

In plants, *TCP15* has multiple functions and is involved in a variety of growth, development, and stress responses, such as seed germination; leaf development; stem elongation; and the response to dehydration, salinity, and cold. In addition, hormones such as GA3 and JA acid, as well as auxin pathways, are also involved [39–41]. We detected the expression of key genes of these biological processes and TCP family downstream genes, as reported in a previous study. To elucidate the function of *FmTCP15* in *F. mandshurica*, an *Agrobacterium*-mediated transient expression system was used [39]. After coculture with *Agrobacterium*, transient overexpression of the *FmTCP15* plant was obtained. The transgenic expression levels of *FmTCP15* and *GFP* were determined by using qRT-PCR, which verified that the transformation was successful (Figure S1). qRT-PCR was used to examine the expression level of downstream genes (Figure 5). The results showed that the development-related genes *FmRGA*, *FmIAA3*, and *FmDAR1* were upregulated (Figure 5). Stress-response genes *FmAOS*, *FmABI5*, and *FmRAP2.1* and the cold regulation gene *FmCBF1* were also significantly upregulated (Figure 5). In addition, the circadian clock gene *FmCCA1* was also upregulated (Figure 5). However, one of the stress-response genes, *FmRAP2.12*, was suppressed (Figure 5). It is noteworthy that *FmTCP2* from class II and *FmTCP14* from class I showed significant upregulated or downregulated expression, respectively (Figure 5). Other genes did not show significant changes. These results indicated that *FmTCP15* directly regulated a series of development-related and abiotic stress-response genes and may act as a key node for developmental and stress responses.

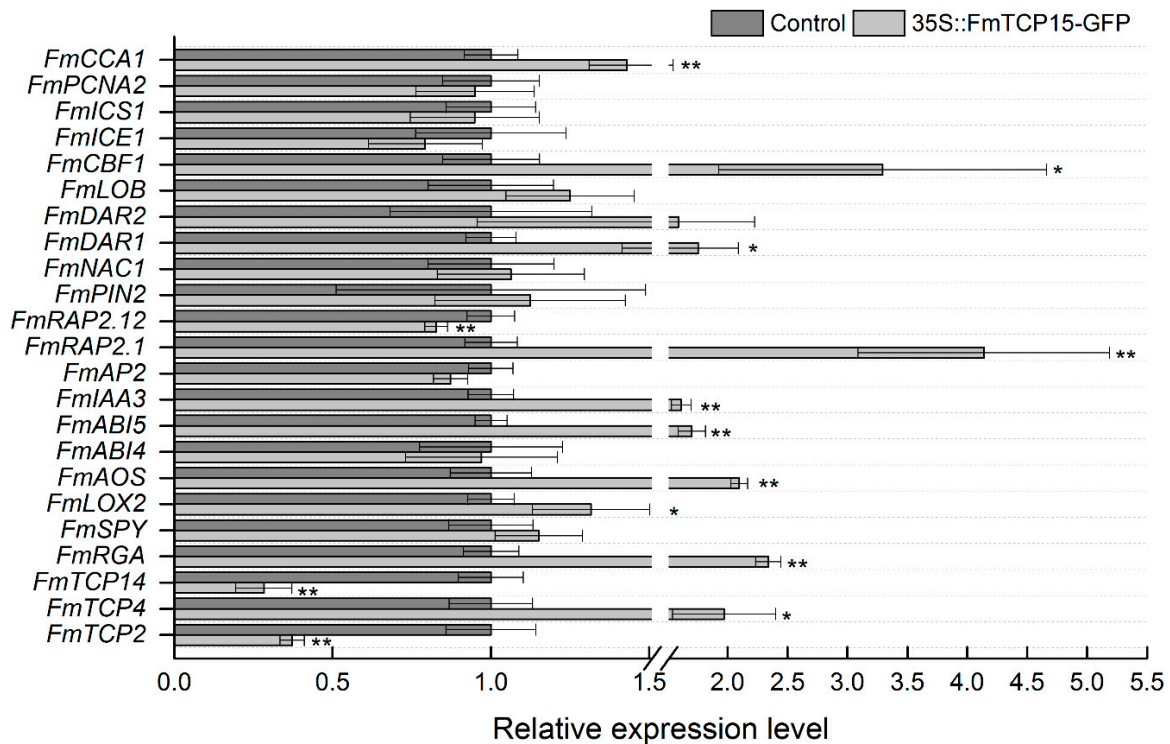


**Figure 5.** Quantitative assay results for downstream genes of transient overexpression of *FmTCP15* seedlings. The expression profile data of downstream genes of *FmTCP15* were obtained through qRT-PCR. \* Indicates a significant difference between control and 35S::*FmTCP15*-GFP ( $p < 0.05$ ). \*\* Indicates a highly significant difference between control and 35S::*FmTCP15*-GFP ( $p < 0.01$ ) according to Duncan's multiple range test.

### 3.6. Protein–Protein Interactions between *FmTCP15* and DELLA Proteins

It is well known that the TCP domain provides TCPs the ability to form homo- and/or heterodimer protein complexes that are involved in the transcriptional activation of a series biological processes [22,42]. Previous studies showed that TCP proteins could interact with DELLA proteins and participate in the GA-regulated signaling regulatory pathway [24]. To determine whether TCP15 directly targets the downstream genes, particularly RGA1 and GAI (i.e., the two DELLA proteins), we conducted a Y2H assays. The full-length coding sequence of *FmTCP15* was recombined into the pGBKT7 (BD) vector and pGADT7 (AD) vector, respectively. The candidate downstream genes of *FmTCP15*, such as *FmRGA*, *FmGAI*, *FmIAA3*, *FmDAR1*, *FmAOS*, *FmABI5*, *FmRAP2.1*, *FmCBF1*, *FmCCA1*, and *FmRAP2.12*, and the other TCP family members, such as *FmTCP2* and *FmTCP14*, were recombined into the pGADT7 (AD) vector. Y2H assays revealed that with the candidate downstream genes, *FmTCP15* could interact with *FmRGA* and *FmGAI* (Figure 6). In addition, *FmTCP15* could also interact with *FmTCP2* from class II and *FmTCP14* from class I (Figure 6). These results indicated that *FmTCP15* proteins interact with DELLA-family proteins and may indirectly respond to stresses throughout the GA-signaling pathway.

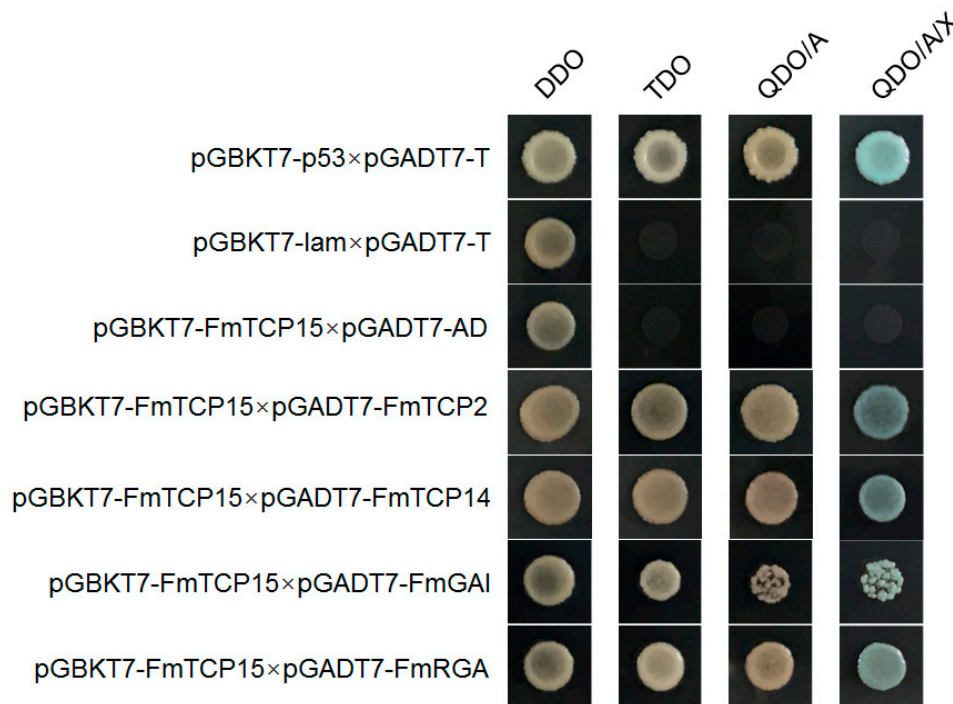


**Figure 6.** Yeast two-hybrid protein–protein interaction assays between FmTCP15 and DELLA proteins. The coding sequences of *FmTCPs*, *FmRGA*, and *FmGAI* were cloned into pGADT7 (AD) and pGBKT7 (BK) vectors. Transformants were assayed for growth on DDO, TDO, QDO/A, and QDO/A/X nutritional selection medium, and turning blue in the presence X- $\alpha$ -Gal was scored as a positive interaction.

#### 4. Discussion

TCP transcription factors are a class of plant-specific transcription factors that play a very important role in many growth processes by directly or indirectly influencing plant hormonal signaling, the cell cycle, and the circadian clock. Research on TCPs has been conducted on various species, but the function of TCP family members in *F. mandshurica* has not been found. In addition, the molecular mechanisms of responses to abiotic stresses, as well as growth and development, in *F. mandshurica* are still scarcely understood. In this study, *FmTCP15* was isolated from *F. mandshurica* and subjected to a detailed bioinformatics analysis. The GO analysis indicated that *FmTCP15* had protein-binding ability and participated multiple biological processes. Homology analysis and a phylogenetic tree of *FmTCP15* revealed that *FmTCP15* was most closely related to the Solanaceae and Plantaginaceae families (Figure 2B).

The tissue-specific expression pattern showed that *FmTCP15* was expressed highest in cotyledons, indicating that *FmTCP15* may play a role in seed germination and seedling development. Subcellular localization showed *FmTCP15* was located in the nucleus. Furthermore, we observed that *FmTCP15* responded to both abiotic stresses and hormone signals. *FmTCP15* was mainly induced by cold, salt, and drought stress treatments and GA3 treatment but downregulated under ABA treatment (Figure 4B–F). Moreover, overexpressing *FmTCP15* caused a significant change in the expression of a series of key genes involved in the GA3, JA acid, and auxin pathways, as well as stress response and the circadian clock (Figure 5). In cotton, overexpression of *GhTCP14* altered the distribution of auxin and upregulated the expression levels of auxin-related genes such as *AUX1*, *PIN2*, and *IAA3* [43]. *IAA3* belongs to the Aux/IAA family and plays very important roles in regulating root growth and lateral root development [44]. A recent study showed that under cold and drought conditions, a series of *MeTCP* genes were significantly upregulated and functioned in resistance to abiotic stresses in cassava [41]. In this study, we found that overexpression of *FmTCP15* increased the expression level of *FmCBF* (Figure 5). The homologous gene of DREB1/CBF in rice has been found to be involved in cold tolerance and chilling acclimation [45]. In response to stress, we found that *FmRAP2.1* and

*FmRAP2.12* were upregulated and downregulated by overexpressed *FmTCP15*, respectively. *RAP2.1* and *RAP2.12* are known as ERF/AP2 transcription factor genes from the ETHYLENE RESPONSE TRANSCRIPTION FACTOR (ERF) family and are involved in oxygen sensing and stress response. In tomato, *SITCP12*, *SITCP15*, and *SITCP18* could bind to AP2/ERF proteins and may be indirectly involved in ethylene-dependent ripening [23]. In a study of *OsTCP19* in rice, a homologous gene of *FmTCP15*, *OsTCP19*, influenced lipid droplet (LD) synthesis and metabolism. In *Arabidopsis*, Rice *OsTCP19* overexpression transgenics upregulated *ABI4* and then promoted the expression of *diacylglycerolacetyl transferase (DGAT1)*, which is a triacylglycerol (TAG) biosynthesis gene that leads to the accumulation of LDs in vegetative tissue [14]. It was reported that TCPs may regulate *CIRCADIAN CLOCK ASSOCIATED1 (CCA1)* and participate in the regulation of the circadian clock. *AtTCP20* and *AtTCP22* acted as coactivators with *LIGHT-REGULATED WD1 (LWD1)* and regulated the expression of *CCA1* in *Arabidopsis* [46]. However, fold changes of *FmTCP15* downstream genes were not very high, which may be related to the transient transformation efficiency not being compared with stable transformation.

Notably, overexpression of *FmTCP15* significantly increased the expression level of *FmRGA* (Figure 6), and the Y2H assay also revealed the protein level interaction between *FmTCP15* and DELLA proteins (*FmRGA* and *FmGAI*) (Figure 6). Our results showed that the regulatory relationship between *FmTCP15* and DELLAs are at the transcriptional and post-transcriptional level. It is well known that the central function of GA3 is to regulate growth and development. However, increasing evidence has shown that GA3 responds to abiotic stresses. Reducing the levels of GA3 or signal transduction will lead to the restriction of plant growth, which is conducive for plant response to cold, salt, and osmotic stresses [47,48]. DELLA proteins are the key regulatory components of the GA-signaling pathway that repress the transcription of GA-responsive genes to restrain plant growth [49–51]. For the stress response, DELLA proteins could mediate the crosstalk between GA and ABA and regulate the balance between seed dormancy and germination [52]. A recent work has shown that during cold temperatures, the transcription of *CBF3* will activate, subsequently decrease the bioactive level of GA3, lead to the accumulation of DELLAs, and thus enhance plant resistance to low temperatures [53]. In *Arabidopsis*, the DELLA protein RGA interacted with the TCP DNA-binding motif of *TCP14* and *TCP15*, negatively controlled the expression of cell-cycle progression genes, and restricted plant height [24]. However, we suspected that the interaction between TCPs and DELLA may enhance plant resistance to stress. We surmised that, on the one hand, *FmTCP15* interacts with DELLA and regulates plant growth, development, and responses to stress by participating in the GA-signaling pathway. On the other hand, *FmTCP15* indirectly regulates downstream abiotic response genes to respond to abiotic stresses. Interestingly, we observed that *FmTCP2* from class II and *FmTCP14* from class I showed significant upregulated or downregulated expression in overexpressing *FmTCP15* plants. In addition, *FmTCP4* from class II was significantly upregulated. Y2H assay also demonstrated the interaction between *FmTCP15*, *FmTCP2*, and *FmTCP14*. These results indicated that there were interactions between classes I and II TCPs, and that the molecular mechanism of TCPs responding to hormone signaling pathways, growth, development, and abiotic stresses is flexible, complex, and multifunctional.

In summary, we revealed that *FmTCP15* was significantly induced by cold, salt, and drought stress and GA3. Overexpressing *FmTCP15* caused a change in the expression of a series of key genes involved in stress response, including *FmRAP2.1*, *FmRAP2.12*, and *FmCBF*; plant growth regulation, including *FmIAA3* and *FmDAR1*; and the GA-signaling pathway genes, including DELLA-family members (*FmRGA* and *FmGAI*), which are key proteins of the GA-signaling pathway. These results showed the *FmTCP15* directly responded to the stresses. Moreover, *FmTCP15* could interact with *FmRGA* and *FmGAI* at the protein level. As previously shown, the DELLA proteins are the key regulatory components of the GA-signaling pathway and restrain plant growth but enhance plant resistance to stress responses. The interactive relationship between *FmTCP15* and DELLA proteins may enhance the ability of plants to resist stress responses, which suggests that its crucial function is indirectly responsive to stresses throughout the GA-signaling pathway. Regarding the gene diversity

functions of the TCP family of genes, in the future, research on the molecular mechanisms of TCPs still needs to be enriched.

## 5. Conclusions

*FmTCP15* encoded a protein of 362 amino acids with a TCP domain. The phylogenetic relationship showed that *FmTCP15* was most closely related to the Solanaceae and Plantaginaceae families. *FmTCP15* was localized in the nuclei and highly expressed in cotyledons. *FmTCP15* was mainly induced by cold, salt, and drought stress and GA3 but downregulated by ABA, revealing the *FmTCP15* response to multiple abiotic stresses and hormone signals. Overexpressing *FmTCP15* caused the expression change of the key genes in the stress and hormone responses and circadian clock. *FmTCP15* interacted with DELLA proteins (*FmGAI* and *FmRGA*). Thus, on the one hand, *FmTCP15* directly regulated the abiotic stress-response genes and responded to stresses. On the other hand, *FmTCP15* interacted with the GA-signaling pathway genes, such as DELLA-family members, and indirectly responded to stresses throughout the GA-signaling pathway and enhanced the ability of the plant to resist stress responses. *FmTCP15* presents a variety of functions, and the molecular mechanism of *FmTCP15* still requires in-depth research.

**Supplementary Materials:** The following are available online at <http://www.mdpi.com/1999-4907/10/4/343/s1>, Figure S1: Quantitative assay results for *GFP* and *FmTCP15* genes in transient overexpression of *FmTCP15* seedlings, Table S1: Primers for quantitative RT-PCR (qRT-PCR), Table S2: Primers for yeast two-hybrid assay (Y2H), Table S3: Amino acid sequences for multiple sequence alignment, Table S4: Amino acid sequences for phylogenetic tree construction.

**Author Contributions:** The experiments were designed by N.L. and Y.Z. The manuscript was written by N.L. The experiments were carried out by N.L., L.Y. and Z.W. The experimental materials were collected by N.L. and L.Y. The manuscript was reviewed and edited by N.L., Y.Z. and F.Z.

**Funding:** This research was funded by a grant from the National Key Research and Development Project of China (No. 2017YFD0600605-01) and the National Natural Science Foundation of China (NSFC) (No. 31270697).

**Conflicts of Interest:** The authors declare no conflict of interest.

## References

1. Luo, D.; Carpenter, R.; Vincent, C.; Copsey, L.; Coen, E. Origin of floral asymmetry in *Antirrhinum*. *Nature* **1996**, *383*, 794–799. [[CrossRef](#)] [[PubMed](#)]
2. Doebley, J.; Stec, A.; Hubbard, L. The evolution of apical dominance in maize. *Nature* **1997**, *386*, 485–488. [[CrossRef](#)] [[PubMed](#)]
3. Cubas, P.; Lauter, N.; Doebley, J.; Coen, E. The TCP domain: A motif found in proteins regulating plant growth and development. *Plant J.* **1999**, *18*, 215–222. [[CrossRef](#)] [[PubMed](#)]
4. Kosugi, S.; Ohashi, Y. PCF1 and PCF2 specifically bind to cis elements in the rice proliferating cell nuclear antigen gene. *Plant Cell.* **1997**, *9*, 1607–1619. [[CrossRef](#)] [[PubMed](#)]
5. Dhaka, N.; Bhardwaj, V.; Sharma, M.K.; Sharma, R. Evolving Tale of TCPs: New Paradigms and Old Lacunae. *Front Plant Sci.* **2017**, *8*, 479. [[CrossRef](#)] [[PubMed](#)]
6. Kosugi, S.; Ohashi, Y. DNA binding and dimerization specificity and potential targets for the TCP protein family. *Plant J.* **2002**, *30*, 337–348. [[CrossRef](#)]
7. Martín-Trillo, M.; Cubas, P. TCP genes: A family snapshot ten years later. *Trends Plant Sci.* **2010**, *15*, 31–39. [[CrossRef](#)] [[PubMed](#)]
8. Navaud, O.; Dabos, P.; Carnus, E.; Tremousaygue, D.; Hervé, C. TCP transcription factors predate the emergence of land plants. *J. Mol. Evol.* **2007**, *65*, 23–33. [[CrossRef](#)]
9. Girardi, C.L.; Rombaldi, C.V.; Dal Cero, J.; Nobile, P.M.; Laurens, F.; Bouzayen, M.; Quecini, V. Genome-wide analysis of the AP2/ERF superfamily in apple and transcriptional evidence of ERF involvement in scab pathogenesis. *Sci. Hort.* **2013**, *151*, 112–121. [[CrossRef](#)]
10. Howarth, D.G.; Donoghue, M.J. Phylogenetic analysis of the “ECE”(CYC/TB1) clade reveals duplications predating the core eudicots. *Proc. Natl. Acad. Sci. USA* **2006**, *103*, 9101–9106. [[CrossRef](#)] [[PubMed](#)]

11. Li, C.; Potuschak, T.; Colón-Carmona, A.; Gutiérrez, R.A.; Doerner, P. *Arabidopsis* TCP20 links regulation of growth and cell division control pathways. *Proc. Natl. Acad. Sci. USA* **2005**, *102*, 12978–12983. [[CrossRef](#)] [[PubMed](#)]
12. Almeida, D.M.; Gregorio, G.B.; Oliveira, M.M.; Saibo, N.J. Five novel transcription factors as potential regulators of OsNHX1 gene expression in a salt tolerant rice genotype. *Plant Mol. Biol.* **2017**, *93*, 61–77. [[CrossRef](#)] [[PubMed](#)]
13. Mukhopadhyay, P.; Tyagi, A.K.; Tyagi, A.K. OsTCP19 influences developmental and abiotic stress signaling by modulating ABI4-mediated pathways. *Sci. Rep.* **2015**, *5*, 9998. [[CrossRef](#)]
14. Palatnik, J.F.; Allen, E.; Wu, X.; Schommer, C.; Schwab, R.; Carrington, J.C.; Weigel, D. Control of leaf morphogenesis by microRNAs. *Nature* **2003**, *425*, 257–263. [[CrossRef](#)]
15. Koyama, T.; Furutani, M.; Tasaka, M.; Ohme-Takagi, M. TCP transcription factors control the morphology of shoot lateral organs via negative regulation of the expression of boundary-specific genes in *Arabidopsis*. *Plant Cell.* **2007**, *19*, 473–484. [[CrossRef](#)]
16. Schommer, C.; Palatnik, J.F.; Aggarwal, P.; Chételat, A.; Cubas, P.; Farmer, E.E.; Nath, U.; Weigel, D. Control of jasmonate biosynthesis and senescence by miR319 targets. *PLoS Biol.* **2008**, *6*, e230. [[CrossRef](#)]
17. Yang, X.; Zhao, X.; Li, C.; Liu, J.; Qiu, Z.; Dong, Y.; Wang, Y. Distinct regulatory changes underlying differential expression of TEOSINTE BRANCHED1-CYCLOIDEA-PROLIFERATING CELL FACTOR genes associated with petal variations in zygomorphic flowers of *Petrocosmea* spp. of the family Gesneriaceae. *Plant Physiol.* **2015**, *169*, 2138–2151. [[PubMed](#)]
18. Gonzalezgrandio, E.; Pozacarrion, C.; Oscar, C.; Sorzano, S.; Cubas, P. BRANCHED1 Promotes Axillary Bud Dormancy in Response to Shade in *Arabidopsis*. *Plant Cell.* **2013**, *25*, 834–850. [[CrossRef](#)]
19. Reddy, S.K.; Holalu, S.V.; Casal, J.J.; Finlayson, S.A. Abscisic acid regulates axillary bud outgrowth responses to the ratio of red to far-red light. *Plant Physiol.* **2013**, *163*, 1047–1058. [[CrossRef](#)] [[PubMed](#)]
20. Guo, S.; Xu, Y.; Liu, H.; Mao, Z.; Zhang, C.; Ma, Y.; Zhang, Q.; Meng, Z.; Chong, K. The interaction between OsMADS57 and OsTB1 modulates rice tillering via DWARF14. *Nat. Commun.* **2013**, *4*, 1566. [[CrossRef](#)]
21. Costa, M.M.R.; Fox, S.; Hanna, A.I.; Baxter, C.; Coen, E. Evolution of regulatory interactions controlling floral asymmetry. *Development* **2005**, *132*, 5093–5101. [[CrossRef](#)] [[PubMed](#)]
22. Danisman, S.; Van der Wal, F.; Dhondt, S.; Waites, R.; de Folter, S.; Bimbo, A.; van Dijk, A.D.; Muino, J.M.; Cutri, L.; Dornelas, M.C. *Arabidopsis* class I and class II TCP transcription factors regulate jasmonic acid metabolism and leaf development antagonistically. *Plant Physiol.* **2012**, *159*, 1511–1523. [[CrossRef](#)]
23. Parapunova, V.; Busscher, M.; Busscher-Lange, J.; Lammers, M.; Karlova, R.; Bovy, A.G.; Angenent, G.C.; de Maagd, R.A. Identification, cloning and characterization of the tomato TCP transcription factor family. *BMC Plant Biol.* **2014**, *14*, 157. [[CrossRef](#)] [[PubMed](#)]
24. Davière, J.M.; Wild, M.; Regnault, T.; Baumberger, N.; Eisler, H.; Genschik, P.; Achard, P. Class I TCP-DELLA interactions in inflorescence shoot apex determine plant height. *Curr. Biol.* **2014**, *24*, 1923–1928. [[CrossRef](#)] [[PubMed](#)]
25. Torres, M.L.D.L.Y.; Palomares, O.; Quiralte, J.; Pauli, G.; Rodriguez, R.; Villalba, M. An Enzymatically Active  $\beta$ -1,3-Glucanase from Ash Pollen with Allergenic Properties: A Particular Member in the Oleaceae Family. *PLoS ONE* **2015**, *10*, e0133066. [[CrossRef](#)] [[PubMed](#)]
26. Song, J.; Yang, D.; Niu, C.; Zhang, W.; Wang, M.; Hao, G. Correlation between leaf size and hydraulic architecture in five compound-leaved tree species of a temperate forest in NE China. *For. Ecol. Manage.* **2017**, *418*, 63–72. [[CrossRef](#)]
27. Gang, Q.; Yan, Q.; Zhu, J. Effects of thinning on early seed regeneration of two broadleaved tree species in larch plantations: Implication for converting pure larch plantations into larch-broadleaved mixed forests. *Forestry* **2015**, *88*, 573–585. [[CrossRef](#)]
28. Huang, S.; Sun, X.; Zhang, Y.; Sun, H.; Wang, Z. Nutrient retranslocation from the fine roots of *Fraxinus mandshurica* and *Larix olgensis* in northeastern China. *J. For. Res.* **2016**, *27*, 1305–1312. [[CrossRef](#)]
29. Li, T.; Wu, J.; Chen, H.; Ji, L.; Yu, D.; Zhou, L.; Zhou, W.; Tong, Y.; Li, Y.; Dai, L. Intraspecific functional trait variability across different spatial scales: A case study of two dominant trees in Korean pine broadleaved forest. *Plant Ecol.* **2018**, *219*, 875–886. [[CrossRef](#)]
30. Drenkhan, R.; Solheim, H.; Bogacheva, A.M.; Riit, T.; Adamson, K.; Drenkhan, T.; Maaten, T.; Hietala, A.M. *Hymenoscyphus fraxineus* is a leaf pathogen of local *Fraxinus* species in the Russian Far East. *Plant Pathol.* **2017**, *66*, 490–500. [[CrossRef](#)]

31. Gasteiger, E.; Hoogland, C.; Gattiker, A.; Duvaud, S.e.; Wilkins, M.R.; Appel, R.D.; Bairoch, A. Protein identification and analysis tools on the ExPASy server. In *The Proteomics Protocols Handbook*, 1st ed.; John, M.W., Ed.; Humana Press: Clifton, NJ, USA, 2005; pp. 571–607.
32. Hofmann, K. TMbase-A database of membrane spanning proteins segments. *Biol. Chem. Hoppe-Seyler*. **1993**, *374*, 166.
33. Wang, Y.; Virtanen, J.; Xue, Z.; Tesmer, J.J.; Zhang, Y. Using iterative fragment assembly and progressive sequence truncation to facilitate phasing and crystal structure determination of distantly related proteins. *Acta Crystallogr. D* **2016**, *72*, 616–628. [[CrossRef](#)] [[PubMed](#)]
34. Wang, Y.; Virtanen, J.; Xue, Z.; Zhang, Y. I-TASSER-MR: Automated molecular replacement for distant-homology proteins using iterative fragment assembly and progressive sequence truncation. *Nucleic Acids Res.* **2017**, *45*, 429–434. [[CrossRef](#)]
35. Xu, D.; Zhang, Y. Improving the physical realism and structural accuracy of protein models by a two-step atomic-level energy minimization. *Biophys. J.* **2011**, *101*, 2525–2534. [[CrossRef](#)]
36. Lin, Y.; Li, W.; Chen, H.; Li, Q.; Sun, Y.; Shi, R.; Lin, C.; Wang, J.P.; Chen, H.; Chuang, L. A simple improved-throughput xylem protoplast system for studying wood formation. *Nat. Protoc.* **2014**, *9*, 2194–2205. [[CrossRef](#)]
37. Zhang, Y.; Wang, Y.; Wang, C. Gene overexpression and gene silencing in Birch using an *Agrobacterium*-mediated transient expression system. *Mol. Biol. Rep.* **2012**, *39*, 5537–5541. [[CrossRef](#)] [[PubMed](#)]
38. Livak, K.J.; Schmittgen, T.D. Analysis of relative gene expression data using real-time quantitative PCR and the  $2^{-\Delta\Delta CT}$  method. *Methods* **2001**, *25*, 402–408. [[CrossRef](#)]
39. Kieffer, M.; Master, V.; Waites, R.; Davies, B. TCP14 and TCP15 affect internode length and leaf shape in *Arabidopsis*. *Plant J.* **2011**, *68*, 147–158. [[CrossRef](#)] [[PubMed](#)]
40. Resentini, F.; Felipo-Benavent, A.; Colombo, L.; Blázquez, M.A.; Alabadí, D.; Masiero, S. TCP14 and TCP15 mediate the promotion of seed germination by gibberellins in *Arabidopsis thaliana*. *Mol. Plant.* **2015**, *8*, 482–485. [[CrossRef](#)]
41. Lei, N.; Yu, X.; Li, S.; Zeng, C.; Zou, L.; Liao, W.; Peng, M. Phylogeny and expression pattern analysis of TCP transcription factors in cassava seedlings exposed to cold and/or drought stress. *Sci. Rep.* **2017**, *7*, 10016. [[CrossRef](#)] [[PubMed](#)]
42. Zhao, J.; Zhai, Z.; Li, Y.; Geng, S.; Song, G.; Guan, J.; Jia, M.; Wang, F.; Sun, G.; Feng, N. Genome-Wide Identification and Expression Profiling of the TCP Family Genes in Spike and Grain Development of Wheat (*Triticum aestivum* L.). *Front Plant Sci.* **2018**, *9*, 1282. [[CrossRef](#)] [[PubMed](#)]
43. Wang, M.; Zhao, P.; Cheng, H.; Han, L.; Wu, X.; Gao, P.; Wang, H.; Yang, C.; Zhong, N.; Zuo, J. The cotton transcription factor TCP14 functions in auxin-mediated epidermal cell differentiation and elongation. *Plant Physiol.* **2013**, *162*, 1669–1680. [[CrossRef](#)]
44. Tian, Q.; Uhlir, N.J.; Reed, J.W. *Arabidopsis* SHY2/IAA3 inhibits auxin-regulated gene expression. *Plant Cell.* **2002**, *14*, 301–319. [[CrossRef](#)] [[PubMed](#)]
45. Mao, D.; Chen, C. Colinearity and similar expression pattern of rice DREB1s reveal their functional conservation in the cold-responsive pathway. *PLoS ONE* **2012**, *7*, e47275. [[CrossRef](#)]
46. Wu, J.; Tsai, H.; Joanito, I.; Wu, Y.; Chang, C.; Li, Y.; Wang, Y.; Hong, J.C.; Chu, J.; Hsu, C.; et al. LWD–TCP complex activates the morning gene CCA1 in *Arabidopsis*. *Nat. Commun.* **2016**, *7*, 13181. [[CrossRef](#)]
47. Colebrook, E.H.; Thomas, S.G.; Phillips, A.; Hedden, P. The role of gibberellin signalling in plant responses to abiotic stress. *J. Exp. Biol.* **2014**, *217*, 67–75. [[CrossRef](#)] [[PubMed](#)]
48. Liu, B.; De Storme, N.; Geelen, D. Cold-Induced Male Meiotic Restitution in *Arabidopsis thaliana* Is Not Mediated by GA-DELTA Signaling. *Front Plant Sci.* **2018**, *9*, 91. [[CrossRef](#)] [[PubMed](#)]
49. Achard, P.; Gong, F.; Cheminant, S.; Alioua, M.; Hedden, P.; Genschik, P. The Cold-Inducible CBF1 Factor–Dependent Signaling Pathway Modulates the Accumulation of the Growth-Repressing DELLA Proteins via Its Effect on Gibberellin Metabolism. *Plant Cell.* **2008**, *20*, 2117–2129. [[CrossRef](#)]
50. King, K.E.; Moritz, T.; Harberd, N.P. Gibberellins Are Not Required for Normal Stem Growth in *Arabidopsis thaliana* in the Absence of GAI and RGA. *Genetics* **2001**, *159*, 767–776. [[PubMed](#)]
51. Yang, D.L.; Yao, J.; Mei, C.S.; Tong, X.H.; Zeng, L.J.; Li, Q.; Xiao, L.T.; Sun, T.; Li, J.; Deng, X.W. Plant hormone jasmonate prioritizes defense over growth by interfering with gibberellin signaling cascade. *Proc. Natl. Acad. Sci. USA* **2012**, *109*, 7152–7153. [[CrossRef](#)]

52. Verma, V.; Ravindran, P.; Kumar, P.P. Plant hormone-mediated regulation of stress responses. *BMC Plant Biol.* **2016**, *16*, 86. [[CrossRef](#)] [[PubMed](#)]
53. Zhou, M.; Chen, H.; Wei, D.; Ma, H.; Lin, J. *Arabidopsis* CBF3 and DELLAs positively regulate each other in response to low temperature. *Sci. Rep.* **2017**, *7*, 39819. [[CrossRef](#)] [[PubMed](#)]



© 2019 by the authors. Licensee MDPI, Basel, Switzerland. This article is an open access article distributed under the terms and conditions of the Creative Commons Attribution (CC BY) license (<http://creativecommons.org/licenses/by/4.0/>).